The 2009 IEEE/RSJ International Conference on
Intelligent Robots and Systems
October 11-15, 2009 St. Louis, USA

Control of the Double-Linked Trident Snake Robot based on the Analysis of its Oscillatory Dynamics

Masato ISHIKAWA and Takahiro FUJINO

Abstract— **In this paper, we propose a new approach to the locomotion control of the *trident snake robot*, focusing on its "double-linked" case where the robot is composed of a triangular body and three branches of double-linked snake-like legs. Originally, this robot was proposed by the authors as a novel example of nonholonomic mobile robot. This robot is quite interesting from a theoretical point of view; the well-known LARC(Lie Algebra Rank Condition) for its nonlinear controllability has a unique structure that it contains two 'generator' vector-fields and higher order Lie brackets, which makes its control problem extremely challenging. In this paper, for this difficult control problem, we first propose a design algorithm which partially achieves the desired locomotion. Then we discover that the resulting motion may or may not be a stable limit cycle, depending on the eigenvalues of the corresponding discrete-time dynamics on its Poincaré map. Finally, we propose a full controller design by combining the stable limit cycles. The validity of the proposed idea is examined by numerical simulations.**

I. INTRODUCTION

The trident snake robot is a novel kind of wheeled mobile robot proposed by the authors [1]. This robot is composed of three branches of serial links and a root block, where the three branches are connected to the root block at center, just like a three-pointed star. Each branch is the same as a conventional snake-like robot: i.e., every link has a passive wheel and all the joints are actuated.

This is quite interesting from a theoretical point of view since the well-known LARC(Lie Algebra Rank Condition, given by Chow's theorem[2]) for its nonlinear controllability has a unique structure (given by eq. (10)). It contains two 'generator' vector-fields as well as higher order Lie brackets, which makes the control problem extremely challenging.

The locomotion principle of the trident snake has been clarified for the single-linked case, by analyzing its controllability structure and corresponding holonomy [3]. Now we proceed to tackle with the double-linked case. Unlike 1-link model, the controllability structure of double-linked model is composed of higher order Lie brackets, whose controllability structure is quite complicated. It also has some physical advantages to the 1-link model, e.g., it seldom falls into singular posture, and each wheel supports less load because the contact force is ditributed to larger numbers of wheels.

In this paper, for this difficult control problem, we first propose a design algorithm which partially achieves the desired locomotion utilizing the principle of holonomy. Then we discover that the resulting motion may or may not be a stable limit cycle, depending on the eigenvalues of the corresponding discrete-time dynamics on its Poincaré map. Finally, we propose a full controller design by incorporating the stable limit cycles. Note that, among a lot of studies on nonhonomic motion planning([4], [5], [6]), gait generation and analysis([7], [8], [9]), an advantage of the proposed method is to focus on the stability of oscillations, and to utilize a relatively simple (first-order) gait to deal with complicated (more than second-order) controllability structure.

This paper is organized as follows. Section II introduces the symbol definitions and the kinematic model of the robot. In Section III, we give its controllability analysis and a fundamental control principle based on the controllability structure and the holonomy generation (so-called Lie bracket motion). The control algorighm for translational locomotion is proposed in Section IV, followed by the shape control (rearrangement of the robot's shape without changing its position) proposed in Section V. Section VI concludes the paper.

M. Ishikawa is with the Department of Systems Science, Graduate School of Informatics, Kyoto university; Gokasho, Uji, 611-0011 Kyoto, Japan masato@i.kyoto-u.ac.jp

T. Fujino is with West Japan Railway Company, Ltd.; 4-24, Kita-ku Shibata 2-chome, Osaka, 530-8341 Osaka, Japan

II. MODELING OF THE TRIDENT SNAKE ROBOT

The following symbols are used throughout the paper: $\mathbb{R}$ denotes the set of all real numbers, $\mathbb{Z}$ denotes the set of all integers, $\mathbb{N}$ denotes the set of all natural numbers and $\mathbb{N}_0 := N \cup \{0\}$ denotes the nonnegative integers. Lie bracket of any two vector-fields $f(\boldsymbol{\xi})$ and $g(\boldsymbol{\xi})$ is given by

$$[f, g](\boldsymbol{\xi}) := \frac{\partial g}{\partial \boldsymbol{\xi}} f(\boldsymbol{\xi}) - \frac{\partial f}{\partial \boldsymbol{\xi}} g(\boldsymbol{\xi}).$$

A. Kinematics of the Robot

Fig. 1 illustrates the overview of the trident snake robot placed on the flat plane. In the middle of its body, the root

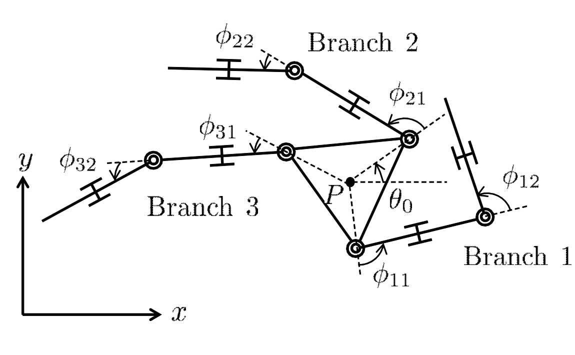

Fig. 1. Model of the double-linked trident snake robot

978-1-4244-3804-4/09/$25.00 ©2009 IEEE

block of the robot is an equilateral triangular plate with three actuated joints at its vertices.

The robot has three branch legs as well, which are connected to the root block via the joints. Each blanch is composed of serial double-link with an actuator at its 'hinge' joint. Each link has a passive wheel on its center, which is assumed not to slip, nor slide sideways. This implies that the motion of each wheel is constrained to parallel translation along the link or spin about its vertical axis.

We assume that the radius of the triangle (the distance between its center and a vertex) is the unit length and all the links are twice as long as the unit, thus the distance between a wheel and its adjacent joint is 1.

The position of the robot is characterized by the coordinates (x, y) of the center P of the root block. The front face of the robot is supposed to be the joint ϕ_{21}, and the orientation of the robot is characterized θ_0. The *configuration* vector of the robot is

$$\boldsymbol{w} := [\ x,\ y,\ \theta_0\ ]^\top \in SE(2)$$

Let ϕ_{ij} denote the j-th joint of the i-th branch. The link between the joints ϕ_{ij} and ϕ_{ij+1} is called the link-(i, j). Now we gather all the 'root' angles into $\boldsymbol{\phi_{\cdot 1}}$, and all the 'hinge' angles into $\boldsymbol{\phi_{\cdot 2}}$, as follows:

$$\boldsymbol{\phi_{\cdot 1}} : = [\ \phi_{11},\ \phi_{21},\ \phi_{31}\ ]^\top$$
$$\boldsymbol{\phi_{\cdot 2}} : = [\ \phi_{12},\ \phi_{22},\ \phi_{32}\ ]^\top$$

Finally, we combine $\boldsymbol{\phi_{\cdot 1}}$ and $\boldsymbol{\phi_{\cdot 2}}$ into the *shape vector* $\boldsymbol{\phi}$:

$$\boldsymbol{\phi} : = [\ \boldsymbol{\phi_{\cdot 1}},\ \boldsymbol{\phi_{\cdot 2}}\ ]^\top$$

Considering the nonholonomic constraints concerning the *non-slide-slip condition* of the wheels, the kinematics of this robot is described as follows:

$$A(\boldsymbol{\phi}) R_{\theta_0}^\top \dot{\boldsymbol{w}} = B(\boldsymbol{\phi}) \dot{\boldsymbol{\phi}} \tag{1}$$

See [3] for the detail of its derivation. Here R_{θ_0} is the homogeneous transformation matrix on $SE(2)$:

$$R_{\theta_0} = \begin{bmatrix} \cos\theta_0 & -\sin\theta_0 & 0 \\ \sin\theta_0 & \cos\theta_0 & 0 \\ 0 & 0 & 1 \end{bmatrix}$$

implying the rotation of the configuration w counter-clockwise by θ_0. $A(\boldsymbol{\phi}) \in \mathbb{R}^{6\times 3}$, $B(\boldsymbol{\phi}) \in \mathbb{R}^{6\times 6}$ are matrix-valued function of the shape $\boldsymbol{\phi}$, while R_{θ_0} depends only on the configuration $\boldsymbol{w}$.

B. State Equation

Now we are ready to convert the kinematics equation into the nonlinear state equation. We define the state vector of the robot as

$$\boldsymbol{\xi} := [\ \boldsymbol{\phi},\ \boldsymbol{w}\ ]^\top \tag{2}$$

while the dimension of state variables is 9. Since the number of nonholonomic constraints is 6 (which equals to the number of the wheels), the velocity $\dot{\boldsymbol{\xi}}$ is confined in a three-dimensional (tangent) subspace at every instance, as far as kinematics is concerned. From control point of view, this implies that we may have only 3 control parameters to specify the velocity $\dot{\boldsymbol{\xi}}$, nevertheless the number of active joints is 6. In this paper, we derive two forms of state equations, depending on the choice of control inputs. We take the base velocity $\dot{\boldsymbol{w}}$ as the control input in the first case, while it is the angular velocity of the root joints $\dot{\boldsymbol{\phi}}_{\boldsymbol{\cdot 1}}$ in the second case. Both cases are essentially equivalent to each other under proper input transformation.

Case 1: Let $\boldsymbol{u} = [\ x,\ y,\ \theta_0\ ]$

From (1), we obtain following state equation

$$\begin{bmatrix} \dot{\boldsymbol{\phi}} \\ \dot{\boldsymbol{w}} \end{bmatrix} = \begin{bmatrix} B(\boldsymbol{\phi})^{-1} A(\boldsymbol{\phi}) R_{\theta_0}^\top \\ I_3 \end{bmatrix} \boldsymbol{u} \tag{3}$$

where I_3 is 3×3 indentity matrix. Then we can rewrite it in the following form

$$\dot{\boldsymbol{\xi}} = \boldsymbol{g_1}(\boldsymbol{\xi}) u_1 + \boldsymbol{g_2}(\boldsymbol{\xi}) u_2 + \boldsymbol{g_3}(\boldsymbol{\xi}) u_3 \tag{4}$$

where $\boldsymbol{g_1} \in \mathbb{R}^{9\times 1}, \boldsymbol{g_2} \in \mathbb{R}^{9\times 1}, \boldsymbol{g_3} \in \mathbb{R}^{9\times 1}$ are smooth vector-fields.

Case2: Let $\boldsymbol{u} = [\ \phi_{11},\ \phi_{21},\ \phi_{31}\ ]$

We divide the 6×6 matrix $B(\boldsymbol{\phi})$ into following block matrix

$$B(\boldsymbol{\phi}) = \begin{bmatrix} B_1(\boldsymbol{\phi}) & B_2(\boldsymbol{\phi}) \end{bmatrix} \tag{5}$$

where $B_1(\boldsymbol{\phi}) \in \mathbb{R}^{6\times 3}, B_2(\boldsymbol{\phi}) \in \mathbb{R}^{6\times 3}$. Using (5), kinematics equation (1) transforms as follows

$$\begin{bmatrix} -B_2(\boldsymbol{\phi}) & A(\boldsymbol{\phi}) R_{\theta_0}^\top \end{bmatrix} \begin{bmatrix} \dot{\boldsymbol{\phi}}_{\boldsymbol{\cdot 2}} \\ \dot{\boldsymbol{w}} \end{bmatrix} = B_1(\boldsymbol{\phi}) \dot{\boldsymbol{\phi}}_{\boldsymbol{\cdot 1}} \tag{6}$$

Then, we can obtain following state equation

$$\begin{bmatrix} \dot{\boldsymbol{\phi}}_{\boldsymbol{\cdot 1}} \\ \dot{\boldsymbol{\phi}}_{\boldsymbol{\cdot 2}} \\ \dot{\boldsymbol{w}} \end{bmatrix} = \begin{bmatrix} I_3 \\ \begin{bmatrix} -B_2(\boldsymbol{\phi}) & A(\boldsymbol{\phi}) R_{\theta_0}^\top \end{bmatrix}^{-1} B_1(\boldsymbol{\phi}) \end{bmatrix} \boldsymbol{u} \tag{7}$$

Now we rewrite it in the vector-field form

$$\dot{\boldsymbol{\xi}} = \boldsymbol{h_1}(\boldsymbol{\xi}) u_1 + \boldsymbol{h_2}(\boldsymbol{\xi}) u_2 + \boldsymbol{h_3}(\boldsymbol{\xi}) u_3 \tag{8}$$

where $\boldsymbol{h_1} \in \mathbb{R}^{9\times 1}, \boldsymbol{h_2} \in \mathbb{R}^{9\times 1}, \boldsymbol{h_3} \in \mathbb{R}^{9\times 1}$ are smooth vector-fields. In summary, both state equations (4) and (8) are 3-input and 9-state drift-free (or symmetric affine) systems.

Remark 1: From now on, we sometimes omit the arguments $\boldsymbol{\xi}$ from the vector-fields $\boldsymbol{g}(\boldsymbol{\xi}), \boldsymbol{h}(\boldsymbol{\xi})$. In addition, we use the notation $\boldsymbol{g^w}, \boldsymbol{h^w} \in \mathbb{R}^{3\times 1}$, $\boldsymbol{g^{\phi_{\cdot 1}}}, \boldsymbol{h^{\phi_{\cdot 1}}} \in \mathbb{R}^{3\times 1}$, $\boldsymbol{g^{\phi_{\cdot 2}}}, \boldsymbol{h^{\phi_{\cdot 2}}} \in \mathbb{R}^{3\times 1}$ to indicate the components of the vector-fields, corresponding velocities of the base, angular velocities of the root and angular velocities of the hinge joint respectively, as follows.

$$\boldsymbol{g} = \begin{bmatrix} \boldsymbol{g^{\phi_{\cdot 1}}} \\ \boldsymbol{g^{\phi_{\cdot 2}}} \\ \boldsymbol{g^w} \end{bmatrix}, \ \boldsymbol{h} = \begin{bmatrix} \boldsymbol{h^{\phi_{\cdot 1}}} \\ \boldsymbol{h^{\phi_{\cdot 2}}} \\ \boldsymbol{h^w} \end{bmatrix} \tag{9}$$

III. Controllability Analysis and the Fundamental Control Principle

A. Controllability Analysis

Consider the set of input vector-fields $G := \{\boldsymbol{g_1}, \boldsymbol{g_2}, \boldsymbol{g_3}\}$. Controllability of symmetric affine systems is completely characterized by controllability Lie algebra, i.e., the smallest distribution $\bar{G}$ that contains G and closed under the Lie bracket operation. The system is controllable if and only if the dimension of $\bar{G}$ coincides with the dimension of state space at all points. This condition is known as LARC(Lie Algebra Rank Condition) given by Chow's theorem[2].

The controllability Lie algebra of the double-linked model is obtained by calculating Lie brackets as follows. Let us compute the first-order Lie brackets

$$\boldsymbol{g_{12}} := [\boldsymbol{g_1}, \boldsymbol{g_2}],\ \boldsymbol{g_{23}} := [\boldsymbol{g_2}, \boldsymbol{g_3}],\ \boldsymbol{g_{31}} := [\boldsymbol{g_3}, \boldsymbol{g_1}].$$

and some of the *second-order Lie brackets*

$$\boldsymbol{g_{121}} := [[\boldsymbol{g_1}, \boldsymbol{g_2}], \boldsymbol{g_1}],\ \boldsymbol{g_{122}} := [[\boldsymbol{g_1}, \boldsymbol{g_2}], \boldsymbol{g_2}],$$
$$\boldsymbol{g_{311}} := [[\boldsymbol{g_3}, \boldsymbol{g_1}], \boldsymbol{g_1}].$$

By complicated but straightforward computation of Lie bracketting, we can check that

$$\bar{G} := \mathrm{span}\{\boldsymbol{g}_1, \boldsymbol{g}_2, \boldsymbol{g}_3, \boldsymbol{g}_{12}, \boldsymbol{g}_{23}, \boldsymbol{g}_{31}, \boldsymbol{g}_{121}, \boldsymbol{g}_{122}, \boldsymbol{g}_{311}\} \quad (10)$$

and $\bar{G}(\boldsymbol{\xi})$ spans full tangent space $\mathbb{R}^9$ for almost all $\boldsymbol{\xi}$, except some singular postures[1], thus the state equation (4) is controllable. Likewise, starting from the set of input vector-fields $H := \{\boldsymbol{h_1}, \boldsymbol{h_2}, \boldsymbol{h_3}\}$, we can also conclude that the state equation (8) is controllable.

B. Periodic Input Design via Exterior Product Equation

We propose a new control design method to realize desired locomotion of the robot by periodic inputs, which moves the state variables to subspace spanned by the first order Lie brackets $\boldsymbol{g}_{12}, \boldsymbol{g}_{23}, \boldsymbol{g}_{31}$.

First, suppose that the control input $\boldsymbol{u} \in \mathbb{R}^{3\times 1}$ is parameterized by the vector $\bar{\boldsymbol{u}} \in \mathbb{R}^2$ and the matrix $K \in \mathbb{R}^{3\times 2}$ as follows:

$$\boldsymbol{u} = \begin{bmatrix} K_{11} & K_{21} \\ K_{12} & K_{22} \\ K_{13} & K_{23} \end{bmatrix} \bar{\boldsymbol{u}} \quad (11)$$

where $K_{1i} \in \mathbb{R}, K_{2i} \in \mathbb{R}$ $(i = 1, 2, 3)$. Geometrically, this implies that $\boldsymbol{u}$ is resticted to the subspace spanned by $\boldsymbol{K_1} := [K_{11}, K_{12}, K_{13}]^T$ and $\boldsymbol{K_2} := [K_{21}, K_{22}, K_{23}]$ with the coefficients $\bar{u}_1, \bar{u}_2$ (See Fig. 2).

When the input $\boldsymbol{u}$ is restricted to this form, the state equation can be reduced to

$$\dot{\boldsymbol{\xi}} = [\ \bar{\boldsymbol{g}}_1\ \bar{\boldsymbol{g}}_2\ ]\ \bar{\boldsymbol{u}} \quad (12)$$

where $\bar{\boldsymbol{g}}_1, \bar{\boldsymbol{g}}_2$ are linear combinations of input vector-fields $\boldsymbol{g_1}, \boldsymbol{g_2}, \boldsymbol{g_3}$ as follows.

$$\bar{\boldsymbol{g}}_1 := \sum_{i=1}^{3} K_{1i}\boldsymbol{g_i}, \quad \bar{\boldsymbol{g}}_2 := \sum_{i=1}^{3} K_{2i}\boldsymbol{g_i} \quad (13)$$

[1]The singularity occurs when $A(\boldsymbol{\phi})$ fails to be full column-rank. See [3] for detailed issue on the singularity.

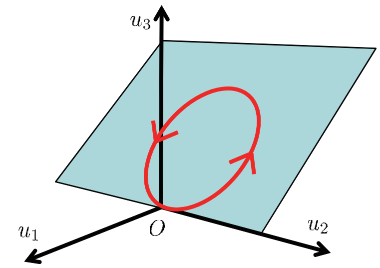

Fig. 2. Cyclic trajectory on the subspace spanned by $\boldsymbol{K_1}, \boldsymbol{K_2}$

Now suppose to apply the following time-periodic signal to $\bar{\boldsymbol{u}}$:

$$\bar{\boldsymbol{u}} = [\ \bar{u}_1,\ \bar{u}_2\ ]^\top = [\ -\epsilon\omega \sin \omega t,\ \epsilon\omega \cos \omega t\ ]^\top \quad (14)$$

then $\boldsymbol{\xi}_T := \boldsymbol{\xi}(T)$ where $T = 2\pi/\omega$, the state after one cycle, is given by the first-order Lie bracket $[\ \bar{\boldsymbol{g_1}},\ \bar{\boldsymbol{g_2}}\ ]$ as follows:

$$\boldsymbol{\xi}_T = \boldsymbol{\xi}_0 + \pi\epsilon^2 [\ \bar{\boldsymbol{g_1}},\ \bar{\boldsymbol{g_2}}\ ] + \boldsymbol{O}(\epsilon^3) \quad (15)$$

This formula is called *the principle of holonomy*, or the area rule[6]. The reminder $\boldsymbol{O}(\epsilon^3)$ tends to be small for high order of $\epsilon 1$. The net displacement of the state is approximated by

$$\boldsymbol{\Delta\xi}_T := \boldsymbol{\xi}_T - \boldsymbol{\xi}_0 \cong \pi\epsilon^2 [\ \bar{\boldsymbol{g_1}},\ \bar{\boldsymbol{g_2}}\ ] \quad (16)$$

Using the skew-symmetry of Lie bracket operation ($[\boldsymbol{f}, \boldsymbol{g}] = -[\boldsymbol{g}, \boldsymbol{f}]$), we have

$$[\ \bar{\boldsymbol{g_1}},\ \bar{\boldsymbol{g_2}}\ ] = \kappa_{12}\boldsymbol{g_{12}} + \kappa_{23}\boldsymbol{g_{23}} + \kappa_{31}\boldsymbol{g_{31}} \quad (17)$$

$$\begin{aligned} \kappa_{12} &:= K_{11}K_{22} - K_{12}K_{21}, \\ \kappa_{23} &:= K_{12}K_{23} - K_{13}K_{22}, \\ \kappa_{31} &:= K_{13}K_{21} - K_{11}K_{23}. \end{aligned}$$

$\boldsymbol{\kappa} := [\kappa_{23}, \kappa_{31}, \kappa_{12}]^\top$ satisfies the following exterior product equation:

$$\boldsymbol{\kappa} = \boldsymbol{K_1} \times \boldsymbol{K_2} \quad (18)$$

Conversely, given $\boldsymbol{\kappa}$, we can always find $\boldsymbol{K_1}$ and $\boldsymbol{K_2}$ which satisfy (18) though the solution is not unique. The corresponding control input is given by (11) and (14).

C. Approximate equilibrium and analysis of its stability

In this subsection, we consider the periodic dynamics of the system (15) under above pre-specified input design method. Let us we approximate displacement of the state by focusing on the influence of first-order Lie brackets. Suppose $\boldsymbol{\Delta\xi}_T$ is given by the approximated formula (16). Then, a state $\boldsymbol{\xi}^*$ that satisfies

$$[\ \bar{\boldsymbol{g_1}},\ \bar{\boldsymbol{g_2}}\ ](\boldsymbol{\xi}^*) = 0 \quad (19)$$

is called an *approximate equilibrium of first-order* .

Next, let us discretize the original continuous-time system with the interval T:

$$\boldsymbol{\xi}[k] := \boldsymbol{\xi}(kT), \qquad k \in \mathbb{N}_0,\ T = 2\pi\omega \quad (20)$$

Then (15) and (16) are expressed by following equation.

$$\begin{array}{c}\boldsymbol{\xi}[k+1] = \boldsymbol{\xi}[k] + \boldsymbol{\Delta}(\boldsymbol{\xi}[k]) \\ \boldsymbol{\Delta}(\boldsymbol{\xi}[k]) \cong \pi\epsilon^2 \left[\ \bar{\boldsymbol{g}_1},\ \bar{\boldsymbol{g}_2}\ \right](\boldsymbol{\xi}[k])\end{array} \tag{21}$$

Finally, linearization of the system (21) in a vicinity of $\boldsymbol{\xi}^*$ is obtained as follows.

$$\boldsymbol{\xi}[k+1] - \boldsymbol{\xi}^* \cong \left(I_9 + \left.\frac{\partial \boldsymbol{\Delta}(\boldsymbol{\xi}[k])}{\partial \boldsymbol{\xi}[k]}\right|_{\boldsymbol{\xi}[k]=\boldsymbol{\xi}^*} \right)(\boldsymbol{\xi}[k] - \boldsymbol{\xi}^*) \tag{22}$$

where $I_9 \in \mathbb{R}^{9\times 9}$ is 9×9 identity matrix.

$\boldsymbol{\xi}^*$ is a locally asymptotically stable equilibrium of the Poincaré map if the spectral radius of

$$A := I + \left.\frac{\partial \boldsymbol{\Delta}(\boldsymbol{\xi}[k])}{\partial \boldsymbol{\xi}[k]}\right|_{\boldsymbol{\xi}[k]=\boldsymbol{\xi}^*}$$

is less than 1.

IV. Control for Translational Locomotion

The purpose of translation control is to change (x, y) without changing the other variables: the change of state variables after one cycle $\boldsymbol{\Delta\xi}_T$ have to satisfy with

$$\boldsymbol{\Delta\xi}_T = [\ 0,\ 0,\ 0,\ 0,\ 0,\ 0,\ \alpha_x,\ \alpha_y,\ 0\ ]^\top \tag{23}$$

where α_x, α_y is constant of translation. In translation control, we take the angular velocities of the root joints for control input, so state equation is (8).

A. The Periodic Input Design Based on Analysis of Stability

Now, the orientation of the robot doesn't change, so without loss of generality, we set $\theta_0 = 0$. Firstly, not caring with the change of the hinge joint angle, we find $[\ \kappa_{12},\ \kappa_{23},\ \kappa_{31}\ ]^\top$ to satisfy with $\boldsymbol{\Delta w}_T = [\ \alpha_x,\ \alpha_y,\ 0\ ]^\top$ from following equation:

$$\begin{bmatrix}\alpha_x \\ \alpha_y \\ 0\end{bmatrix} = \pi\epsilon^2 \left[\boldsymbol{h}^{\boldsymbol{w}}_{\boldsymbol{12}}(\boldsymbol{\phi})\ \boldsymbol{h}^{\boldsymbol{w}}_{\boldsymbol{23}}(\boldsymbol{\phi})\ \boldsymbol{h}^{\boldsymbol{w}}_{\boldsymbol{31}}(\boldsymbol{\phi})\right] \begin{bmatrix}\kappa_{12} \\ \kappa_{23} \\ \kappa_{31}\end{bmatrix} \tag{24}$$

where $\boldsymbol{h}^{\boldsymbol{w}}_{\boldsymbol{12}}(\boldsymbol{\phi}), \boldsymbol{h}^{\boldsymbol{w}}_{\boldsymbol{23}}(\boldsymbol{\phi}), \boldsymbol{h}^{\boldsymbol{w}}_{\boldsymbol{31}}(\boldsymbol{\phi})$ depends on only the root joint angle $\boldsymbol{\phi_{.1}}$. Furthermore, rank$[\boldsymbol{h}^{\boldsymbol{w}}_{\boldsymbol{12}}(\boldsymbol{\phi}), \boldsymbol{h}^{\boldsymbol{w}}_{\boldsymbol{23}}(\boldsymbol{\phi}), \boldsymbol{h}^{\boldsymbol{w}}_{\boldsymbol{31}}(\boldsymbol{\phi})]^\top = 3$ for arbitrary $\boldsymbol{\phi_{.1}}$, so we can obtain $\boldsymbol{h}^{\boldsymbol{w}}_{\boldsymbol{12}}(\boldsymbol{\phi}), \boldsymbol{h}^{\boldsymbol{w}}_{\boldsymbol{23}}(\boldsymbol{\phi}), \boldsymbol{h}^{\boldsymbol{w}}_{\boldsymbol{31}}(\boldsymbol{\phi})$ uniquely. Under the pre-specified $\kappa_{12}, \kappa_{23}, \kappa_{31}$, the change of the hinge joint angle $\boldsymbol{\Delta\phi_{.2}}$ is expressed as

$$\boldsymbol{\Delta\phi_{.2}} \cong \pi\epsilon^2 \left[\boldsymbol{h}^{\boldsymbol{\phi_{.2}}}_{\boldsymbol{12}}(\boldsymbol{\phi})\ \boldsymbol{h}^{\boldsymbol{\phi_{.2}}}_{\boldsymbol{23}}(\boldsymbol{\phi})\ \boldsymbol{h}^{\boldsymbol{\phi_{.2}}}_{\boldsymbol{31}}(\boldsymbol{\phi})\right] \begin{bmatrix}\kappa_{12} \\ \kappa_{23} \\ \kappa_{31}\end{bmatrix} \tag{25}$$

Here, $\boldsymbol{\phi^*_{.2}}$ satisfying with $\boldsymbol{\Delta\phi_{.2}} = \boldsymbol{0}$ is *the approximate equilibrium of first-order* for $\boldsymbol{\phi_{.2}}$ under pre-specified $\boldsymbol{\phi_{.1}}$ and $\boldsymbol{\kappa}$. Furthermore, analyzing the stability of $\boldsymbol{\phi^*_{.2}}$, we can know the convergent shape of the hinge joint angle for translation.

[Procedure 1] Control input design for translation
Step **1** From (24), set $\kappa_{12}, \kappa_{23}, \kappa_{31}$ for pre-spcified $\boldsymbol{\phi_{.1}}$.
Step **2** Solve $\boldsymbol{\Delta\phi_{.2}} = \boldsymbol{0}$ in (25) to obtain *the approximate equilibrium of first-order:* $\boldsymbol{\phi^*_{.2}}$ and analyze the stability of $\boldsymbol{\phi^*_{.2}}$ to know the convergent shape of the hinge joint angle for translation.
Step **3** Solve $\boldsymbol{K_1}, \boldsymbol{K_2}$ in (**??**) and (**??**).
Step **4** Determine control input $\boldsymbol{u}$ from (11).

B. Simulation

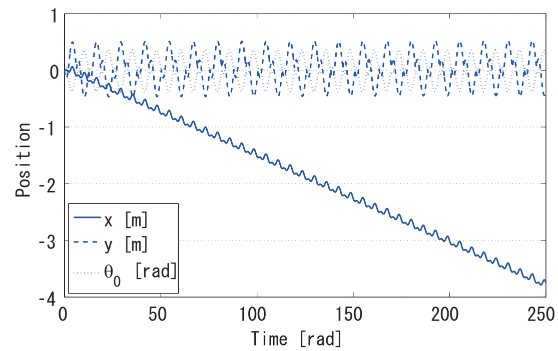

(a)Response of the location

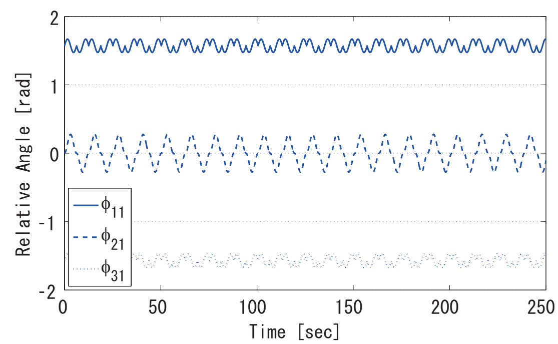

(b)Response of the root joint angles

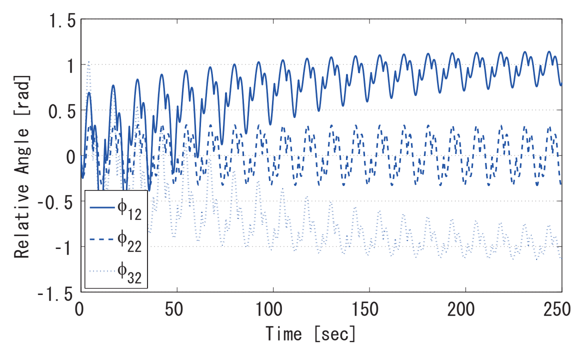

(c)Response of the hinge joint angles

Fig. 3. Simulation results(Translation)

We set $\epsilon = 0.2$, $\omega = 1$ and $\alpha_x = 1, \alpha_y = 0$. In the Step **1**, we obtain $\kappa_{12} = 0.34, \kappa_{23} = -0.34, \kappa_{31} = 0$ from (24) for initial shape $\boldsymbol{\phi}_0 = [\frac{\pi}{2}, 0, -\frac{\pi}{2}, 0, 0, 0]^\top$. In the next Step **2**, we set $\boldsymbol{K_1} = [0, -0.69, 0]^\top, \boldsymbol{K_2} = [0.49, 0, 0.49]^\top$, then the control input for translate from (24) is

$$\begin{cases} u_1 = 0.49\cos t \\ u_2 = 0.69\sin t \\ u_3 = 0.49\cos t \end{cases} \tag{26}$$

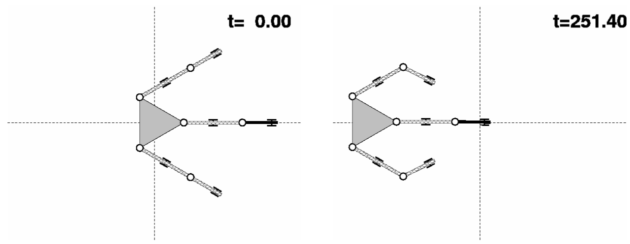

(a)Initial Posture (b)Final Posture

Fig. 4. Simulation results(Translation)

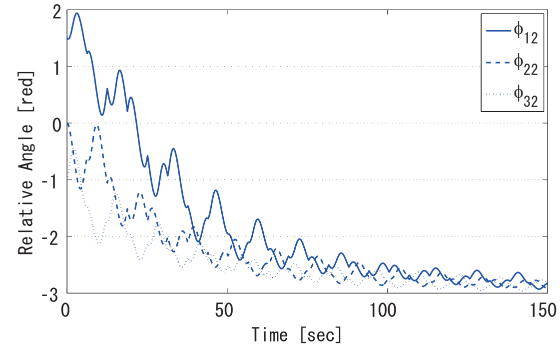

Fig. 5. Convergence of the hinge joint angles to a stable equilibrium

Fig. 3 and Fig. 4 show the simulation results. In Fig. 3, (a) shows the time response of the configuration of the robot: x, y, θ_0. And (b) and (c) show the time response of the root joint angle: $\phi_{11}, \phi_{21}, \phi_{31}$ and the hinge joint angle: $\phi_{12}, \phi_{22}, \phi_{32}$ respectively. From (a), we can confirm that y and θ_0 after one cycle return to initial value, but by contrast, x moves along x-axis to the minus direction. (b) shows that the root joint angle $\dot{\boldsymbol{\phi}}_{\boldsymbol{.1}}$ doesn't change periodically. This is because we take $\dot{\boldsymbol{\phi}}_{\boldsymbol{.1}}$ to control input and apply it periodic function. Furthermore, we can confirm that the hinge joint angle $\boldsymbol{\phi}_{\boldsymbol{.2}}$ converges to a specific value, which is attributed to the stability of *the approximate equilibrium of first-order* $\boldsymbol{\phi}^*_{\boldsymbol{.2}} := [\phi^*_{12}, \phi^*_{22}, \phi^*_{32}]^\top = [1.05, 0, -1.05]^\top$.

V. Control for Shape Rearrangement

The purpose of shape control is to change an initial shape $\boldsymbol{\phi}[0]$ to arbitrary reference shape $\boldsymbol{\phi}^{\mathbf{ref}}$ without changing the configuration vector $\boldsymbol{w}$: the change of state variables after one cycle $\boldsymbol{\Delta\xi}_T$ have to satisfy with

$$\boldsymbol{\Delta\xi}_T = \left[\phi_{11}^{\mathrm{ref}}, \phi_{21}^{\mathrm{ref}}, \phi_{31}^{\mathrm{ref}}, \phi_{12}^{\mathrm{ref}}, \phi_{22}^{\mathrm{ref}}, \phi_{32}^{\mathrm{ref}}, x[0], y[0], \theta_0[0]\right]^\top \tag{27}$$

where $x[0], y[0], \theta_0[0]$ is an initial shape. In shape control, we take the velocities of the base for control input, so state equation is (4).

A. The Existance of Stable Equilibrium and The Definition of Invariant Sets

The orientation of the robot doesn't change, so without loss of generality, we set $\theta_0 = 0$. Now, $\boldsymbol{g}_{\boldsymbol{21}}^{\boldsymbol{\phi}_{\boldsymbol{.1}}}, \boldsymbol{g}_{\boldsymbol{23}}^{\boldsymbol{\phi}_{\boldsymbol{.1}}}, \boldsymbol{g}_{\boldsymbol{31}}^{\boldsymbol{\phi}_{\boldsymbol{.1}}}$ are constant vectors and are linear independent. Therefore, we can set a constant vector $[\kappa_{12}, \kappa_{23}, \kappa_{31}]^\top$ to realize aribitrary change of shape $\boldsymbol{\Delta\phi}_{\boldsymbol{.1}}$ from following equation:

$$\boldsymbol{\Delta\phi}_{\boldsymbol{.1}} = \pi\epsilon^2(\kappa_{12}\boldsymbol{g}_{\boldsymbol{12}}^{\boldsymbol{\phi}_{\boldsymbol{.1}}} + \kappa_{23}\boldsymbol{g}_{\boldsymbol{23}}^{\boldsymbol{\phi}_{\boldsymbol{.1}}} + \kappa_{31}\boldsymbol{g}_{\boldsymbol{31}}^{\boldsymbol{\phi}_{\boldsymbol{.1}}}) \tag{28}$$

Then, under the pre-specified $[\kappa_{12}, \kappa_{23}, \kappa_{31}]^\top$, the change of the hinge joint angles is expressed as follows:

$$\boldsymbol{\Delta\phi}_{\boldsymbol{.2}} \cong \pi\epsilon^2(\kappa_{12}\boldsymbol{g}_{\boldsymbol{12}}^{\boldsymbol{\phi}_{\boldsymbol{.2}}} + \kappa_{23}\boldsymbol{g}_{\boldsymbol{23}}^{\boldsymbol{\phi}_{\boldsymbol{.2}}} + \kappa_{31}\boldsymbol{g}_{\boldsymbol{31}}^{\boldsymbol{\phi}_{\boldsymbol{.2}}}) \tag{29}$$

Fig. 5 shows the time response of the hinge joint angles under pre-specified $\kappa_{12} = 0.5, \kappa_{23} = 0, \kappa_{31} = 0$ in (29). We can confirm that the hinge joint angles converge in a specific value with time, which is due to the stable equibrium existing at the vicinity of the approximate equibrium $-\pi$. As Fig. 5, the hinge joint angles converge to a stable equibrium quickly in initial stage, but decay gradually. Furthermore, we can regard all hinge joint angles as the almost same value over time even if the initial values of them are different from each other. Then, we call the almost same value *the vicinity shape of the stable equibrium* and describe as follows:

$$\boldsymbol{\phi}^{\#}_{\boldsymbol{.2}} := [\ \phi^{\#}_{12},\ \phi^{\#}_{22},\ \phi^{\#}_{32}\ ]^\top \tag{30}$$

Now, we define following set $\boldsymbol{M_1}$ for $(\boldsymbol{\phi}_{\boldsymbol{.1}}, \boldsymbol{\phi}_{\boldsymbol{.2}})$.

$$\boldsymbol{M_1} := \left\{(\boldsymbol{\phi}_{\boldsymbol{.1}},\ \boldsymbol{\phi}_{\boldsymbol{.2}}) \,\middle|\, \boldsymbol{\phi}_{\boldsymbol{.2}} = \boldsymbol{\phi}^{\#}_{\boldsymbol{.2}}\right\} \tag{31}$$

$\boldsymbol{M_1}$ is an invariant set because if $(\boldsymbol{\phi}_{\boldsymbol{.1}}[\ell],\ \boldsymbol{\phi}_{\boldsymbol{.2}}[\ell]) \in \boldsymbol{M_1}$ for $\exists \ell \in \mathbb{N}_0$, then $(\boldsymbol{\phi}_{\boldsymbol{.1}}[\ell+n], \boldsymbol{\phi}_{\boldsymbol{.2}}[\ell+n]) \in \boldsymbol{M_1}$ for $\forall n \in \mathbb{N}$.

Next, we define following set $\boldsymbol{M_2}$ for $(\boldsymbol{\phi}_{\boldsymbol{.1}}, \boldsymbol{\phi}_{\boldsymbol{.2}})$.

$$\boldsymbol{M_2} := \left\{(\boldsymbol{\phi}_{\boldsymbol{.1}},\ \boldsymbol{\phi}_{\boldsymbol{.2}}) \,\middle|\, \boldsymbol{\phi}_{\boldsymbol{.1}} = \boldsymbol{\phi}^{\mathbf{ref}}_{\boldsymbol{.1}} - \boldsymbol{D_k}(\boldsymbol{\phi}^{\mathbf{ref}}_{\boldsymbol{.2}},\ \boldsymbol{\phi}_{\boldsymbol{.2}}), k \in \mathbb{Z}\right\} \tag{32}$$

where $\boldsymbol{D_k}(\boldsymbol{\phi}^{\mathbf{ref}}_{\boldsymbol{.2}}, \boldsymbol{\phi}_{\boldsymbol{.2}})$ is the amount of displacement of $\boldsymbol{\phi}_{\boldsymbol{.1}}$ which we control $\boldsymbol{\phi}_{\boldsymbol{.2}}$ to $\boldsymbol{\phi}^{\mathbf{ref}}_{\boldsymbol{.2}}$ after k cycles as follows:

$$\boldsymbol{D_k}(\boldsymbol{\phi}^{\mathbf{ref}}_{\boldsymbol{.2}}, \boldsymbol{\phi}_{\boldsymbol{.2}}) \cong \pi\epsilon^2 \sum_{\ell=1}^{k} [\ \boldsymbol{g}_{\boldsymbol{12}}^{\boldsymbol{\phi}_{\boldsymbol{.1}}}\ \ \boldsymbol{g}_{\boldsymbol{23}}^{\boldsymbol{\phi}_{\boldsymbol{.1}}}\ \ \boldsymbol{g}_{\boldsymbol{31}}^{\boldsymbol{\phi}_{\boldsymbol{.1}}}\ ]\boldsymbol{\kappa}[\ell] \tag{33}$$

where $\boldsymbol{\kappa}[\ell]$ can be solved from following equation:

$$\boldsymbol{\kappa}[\ell] \cong \frac{1}{\pi\epsilon^2 n}\Big[\boldsymbol{g}_{\boldsymbol{12}}^{\boldsymbol{\phi}_{\boldsymbol{.2}}}(\boldsymbol{\phi}_{\boldsymbol{.2}}[\ell-1])\ \boldsymbol{g}_{\boldsymbol{23}}^{\boldsymbol{\phi}_{\boldsymbol{.2}}}(\boldsymbol{\phi}_{\boldsymbol{.2}}[\ell-1])$$
$$\boldsymbol{g}_{\boldsymbol{31}}^{\boldsymbol{\phi}_{\boldsymbol{.2}}}(\boldsymbol{\phi}_{\boldsymbol{.2}}[\ell-1])\Big]^{-1}(\boldsymbol{\phi}^{\mathbf{ref}}_{\boldsymbol{.2}} - \boldsymbol{\phi}^{\#}_{\boldsymbol{.2}}) \tag{34}$$

(34) is the design equation for $\kappa_{12}[\ell], \kappa_{23}[\ell], \kappa_{31}[\ell]$ to control $\boldsymbol{\phi}_{\boldsymbol{.2}}$ to $\boldsymbol{\phi}^{\mathbf{ref}}_{\boldsymbol{.2}}$ after k cycles and make the amount of displacement after one cycle equal. In fact, if $\boldsymbol{\phi} \in \boldsymbol{M_2}$, then we can control $\boldsymbol{\phi}_{\boldsymbol{.2}}$ to $\boldsymbol{\phi}^{\mathbf{ref}}_{\boldsymbol{.2}}$ and $\boldsymbol{\phi}_{\boldsymbol{.1}}$ to $\boldsymbol{\phi}^{\mathbf{ref}}_{\boldsymbol{.1}}$ simultaneously under pre-specified $\kappa_{12}[\ell], \kappa_{23}[\ell], \kappa_{31}[\ell]$ in (34). Furthermore, as long as we set $\kappa_{12}[\ell], \kappa_{23}[\ell], \kappa_{31}[\ell]$ in (34), if $(\boldsymbol{\phi}_{\boldsymbol{.1}}[\ell], \boldsymbol{\phi}_{\boldsymbol{.2}}[\ell]) \in \boldsymbol{M_2}$ for $\exists \ell \in \mathbb{N}_0$, then $(\boldsymbol{\phi}_{\boldsymbol{.1}}[\ell+n], \boldsymbol{\phi}_{\boldsymbol{.2}}[\ell+n]) \in \boldsymbol{M_2}$ for $\forall n \in \mathbb{N}$, so the set $\boldsymbol{M_2}$ is an invariant set.

B. Periodic Input Design Using Invariant Sets

In this section, we describe about the method of control design using $\boldsymbol{M_1}, \boldsymbol{M_2}$ effectively. If $\boldsymbol{\phi} := (\boldsymbol{\phi}_{\boldsymbol{.1}},\ \boldsymbol{\phi}_{\boldsymbol{.2}})$ belongs to $\boldsymbol{M_2}$, we can control $\boldsymbol{\phi}$ to $\boldsymbol{\phi}^{\mathbf{ref}}$ by setting $\kappa_{12}[\ell], \kappa_{23}[\ell], \kappa_{31}[\ell]$ in (34). Therefore, we have only to

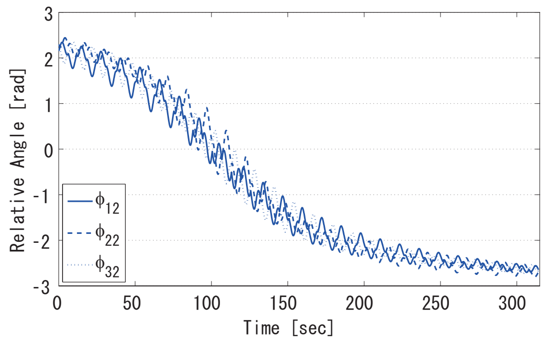

(b)Response of the hinge joint angles

Fig. 6. Shape control (1st step, $\boldsymbol{\phi}[0] \rightarrow \boldsymbol{\phi}^{\boldsymbol{M}}$)

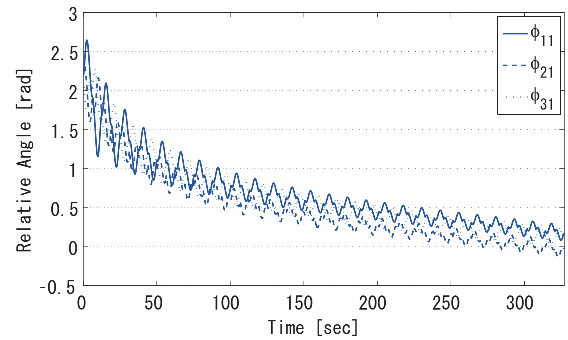

(a)Response of the root joint angles

Fig. 7. Shape Control (2nd step, $\boldsymbol{\phi}^{\boldsymbol{M}} \rightarrow \boldsymbol{\phi}^{\mathbf{ref}}$)

control initial shape $(\boldsymbol{\phi}_{\cdot\mathbf{1}}[0],\ \boldsymbol{\phi}_{\cdot\mathbf{2}}[0])$ to $(\boldsymbol{\phi}_{\cdot\mathbf{1}}^{\boldsymbol{M}_\mathbf{2}},\ \boldsymbol{\phi}_{\cdot\mathbf{2}}^{\boldsymbol{M}_\mathbf{2}}) \in \boldsymbol{M}_\mathbf{2}$. Here, we define a following set:

$$\boldsymbol{M} := \boldsymbol{M}_\mathbf{1} \cap \boldsymbol{M}_\mathbf{2} \tag{35}$$

We can set $\kappa_{12}, \kappa_{23}, \kappa_{31}$ in (28) to control $\boldsymbol{\phi}_{\cdot\mathbf{1}}[0]$ to $\boldsymbol{\phi}_{\cdot\mathbf{1}}^{\boldsymbol{M}} \in \boldsymbol{M}$ and under such a $\kappa_{12}, \kappa_{23}, \kappa_{31}$ it can be expected that $\boldsymbol{\phi}_{\cdot\mathbf{2}}$ converges to the vicinity of $\boldsymbol{\phi}_{\cdot\mathbf{2}}^{\#}$ as Fig. 5 shown. So we can control $\boldsymbol{\phi}$ to $\boldsymbol{\phi}^{\boldsymbol{M}} \in \boldsymbol{M}$ along $\boldsymbol{M}_\mathbf{1}$. Finaly, we swich a control method and control $\boldsymbol{\phi}$ to $\boldsymbol{\phi}^{\mathbf{ref}}$ along $\boldsymbol{M}_\mathbf{2}$.

[Procedure 2] Control input design for shape control

Step **1** Set $\boldsymbol{\phi}_{\cdot\mathbf{2}}^{\#}$ and solve $\boldsymbol{\kappa}[\ell](1 \leq \ell \leq k, \ell \in \mathbb{N})$ from (34)

Step **2** Set $\boldsymbol{D}_{\boldsymbol{k}}(\phi_{\cdot 2}^{\mathrm{ref}}, \phi_{\cdot 2}^{\#})$ from (33)

Step **3** Set $\kappa_{12}, \kappa_{23}, \kappa_{31}$ from (28) and determine control input $\boldsymbol{u}$ form (**??**), (**??**) and (11) to control $\boldsymbol{\phi}$ to $\boldsymbol{\phi}^{\boldsymbol{M}}$

Step **4** Determine the control input $\boldsymbol{u}$ from (11) and (18) using $\boldsymbol{\kappa}[\ell]$ obtained in Step **1**, to change $\boldsymbol{\phi}$ from $\boldsymbol{\phi}^{\boldsymbol{M}}$ to $\boldsymbol{\phi}^{\mathbf{ref}}$.

C. Simulation

We set the initial shape $\phi_0 = [-0.7, -1.0, -0.8, 2.2, 2.3, 2.2]^\top$, the reference shape $\boldsymbol{\phi}^{\mathbf{ref}} = [0, 0, 0, 0, 0, 0]^\top$, $\epsilon = 0.1$, $\omega = 1$ and $\boldsymbol{\phi}_{\cdot\mathbf{2}}^{\#} = -2.7$. Fig. 6 shows the simulation results at Step **3** and Fig. 7 shows the simulation results at Step **4**. Finally, Fig. 8 shows initial posture and final posture of the robot. From Fig. 7, we can confirm that the shape of the robot is controlled to the reference shape.

VI. Conclusions

In this paper, we proposed a new contol method for locomotion control problem of the double-linked trident snake robot. The feature of our proposed method is not to create the behavior corresponding high order Lie brackets which characterize controllability structure of the robot but to use a specific nonlinear dynamics effectively. In the case of this robot, a specific dynamics is the periodical property that some state variables whose behavior can't be designed directly, the hinge joint angles, converge to a stable cycle under pre-specified control prameter. This proposed idea can be a practical control method not only for this robot but also for such a nonlinear system, whose controllable structure is complicated, as multi-generater system.

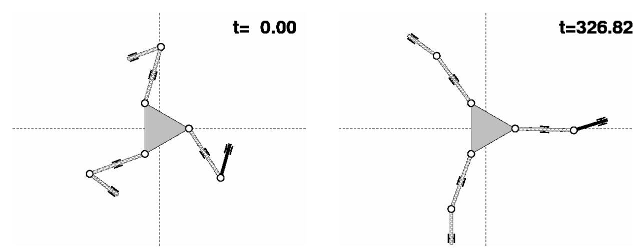

(a)Initial Posture (b)Final Posture

Fig. 8. Shape Control

Acknowledgements

The authors are grateful to Professor Toshiharu Sugie in Kyoto University for his valuable comments and continuous encouragements. This research was supported in part by the Grant-in-Aid for Young Scientists (B), No.19760285 of the Ministry of Education, Science, Sports and Culture, Japan, 2007–2009.

References

[1] M. Ishikawa, Y. Minami, and T. Sugie. Development and control experiment of the trident snake robot(to appear). *IEEE/ASME Transaction on Mechatronics*, 2009.

[2] H. Nijmeijer and A.J. van der Schaft. *Nonlinear Dynamical Control Systems*. Springer Verlag, 1990.

[3] M. Ishikawa. Trident snake robot: Locomotion analysis and control. In *IFAC NOLCOS*, pages 1169–1174, 2004.

[4] R.M Murray and S.S. Sastry. Nonholonomic motion planning: Steering using sinusoids. *IEEE Trans. on Automatic Control*, 38(5):700–716, 1993.

[5] R. Mukherjee and D.P. Anderson. Nonholonomic motion planning using stokes's theorem. In *Proc. of 1993 IEEE Intl. Conf. on Robotics and Automation*, pages 802–809, 1993.

[6] N.E. Leonard and P.S. Krishnaprasad. Motion control of drift-free, left-invariant systems on lie groups. *IEEE Trans. on Automatic Control*, 40(9), 1995.

[7] J. Ostrowski and J. Burdick. The geometric mechanics of undulatory robotic locomotion. *The International Journal of Robotics Research*, 17(7):683–701, 1998.

[8] J. Ostrowski. Steering for a class of dynamic nonholonomic systems. *IEEE Trans. on Automatic Control*, 45(8):1492–1498, 2000.

[9] K.A. McIsaac and J.P. Ostrowski. A framework for steering dynamic robotic locomotion systems. *The International Journal of Robotics Research*, 22:83–97, 2003.